2. In analyzing the efficiency or the overall working capacity of MHD converters with a localized discharge, for the worst (in the mechanical sense) variant the model corresponding to isentropic flow past the discharge with negligibly small thermal wake ($A_1/A_0 \to 1$) can be studied. In this case it is assumed that the size of the discharge is comparable to the transverse size of the channel. The best variant is the plasma-piston model. In the case of a polyatomic molecular gas (in particular, CO_2) for $IBh/A_0p_\infty \gtrsim 10$-15 both models are virtually identical.

3. The comparison of the experimental and computed values of the velocities of the discharge in the "railtron" made above shows that the experimental points fall into the indicated interval, approaching one or another limiting case depending on the conditions and type of gas.

We thank V. S. Sokolov, O. G. Parfenov, V. S. Slavin, and A. D. Lebedev for useful discussions and remarks in the course of this work.

LITERATURE CITED

1. V. A. Derevyanko, V. S. Slavin, and V. S. Sokolov, "Magnetohydrodynamic electricity generator based on the products of gasification of lignite," Zh. Prikl. Mekh. Tekh. Fiz., No. 5 (1980).
2. B. W. Boreham, "Study of traveling conduction wave accelerator," AIAA J., 14, No. 1 (1976).
3. S. A. Belyaev, D. A. Gol'dina, et al., "Calculation of the nonstationary acceleration of plasma in the uniform approximation," Preprint of the Institute of Applied Mathematics of the USSR Academy of Sciences, No. 53 (1969).
4. S. V. Kukhtetskii, V. A. Lyubochko, and A. D. Lebedev, "Some features of the motion of a strong-current quasistationary discharge in a magnetic field," in: Abstracts of Reports at the 9th All-Union Conference on Low-Temperature Plasma Generators [in Russian], Ilim, Frunze (1983).
5. G. Shlikhting, Boundary-Layer Theory [in Russian], Nauka, Moscow (1974).
6. L. G. Loitsyanskii, Mechanics of Liquids and Gases [in Russian], Nauka, Moscow (1970).

DYNAMICS OF LIQUID FILMS. PLANE FILMS WITH FREE RIMS

V. M. Entov, A. N. Rozhkov,
U. F. Feizkhanov, and A. L. Yarin

UDC 532.522+532.62+532.135

The discharge of a liquid from thin slits of finite length ("slit nozzles or dies") results in the formation of characteristic V-shaped plane streams (free dynamic films) which are bounded by free "rims" — boundary streams [1] (Fig. 1a). A similar flow is realized in purer form if a small section is cut out from the dynamic film created, for example, in the flow of a stream against a barrier. Here, the section is isolated by placing two thin blades or wires in the path of the liquid [2]. It is clear that the form of the film and the velocity field in it contain information on the stress field, and quantitative analysis of such flows may be a means of studying the rheology of the liquid. Along with this, it is important to analyze flow in films and in the free rims at their edges to understand the conditions of fragmentation and atomization of the liquid. Presented below are results of theoretical and experimental studies of free films with boundary streams for ideal and viscoelastic liquids.

1. Formulation of the Problem. Taking advantage of the thinness of the film and boundary stream, we can describe the flow as a combination of two-dimensional equations in the region G occupied by the film and one-dimensional "stream" equations on the axis S of the boundary stream. The boundary stream is distinguished from the rest of the liquid by the fact that mass and momentum exchange occur on the lateral surface of the stream. The motion of liquid in the film and rim is conveniently described in polar coordinates (r, θ) in the middle plane of the film. We will examine small segments ABB'A' of a free rim on the edge

Moscow. Translated from Zhurnal Prikladnoi Mekhaniki i Tekhnicheskoi Fiziki, No. 1, pp. 47-53, January-February, 1986. Original article submitted October 10, 1984.

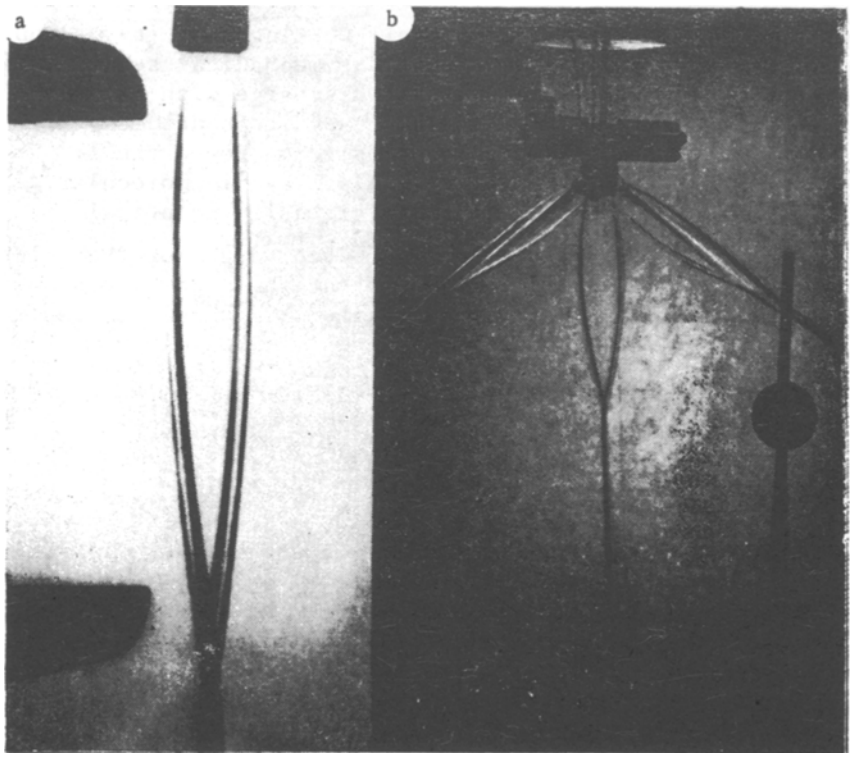

Fig. 1

of a stationary plane film G (Fig. 2), here assuming that flow in the free rim is quasi-unidimensional. This is equivalent to assuming that liquid entering the rim from the film G through the boundary A'B' is instantaneously mixed with the liquid moving inside the rim. In the isolated segment of the rim, a mass of liquid equal to the following moves into areas AA' and A'B' during the time dt

$$\rho (V_\xi f)|_{AA'} dt + \rho (V_r \sin\psi + V_\theta \cos\psi) h|_{A'B'} d\xi\, dt,$$

and moves out of the area BB' $-\ \rho(V_\xi f)|_{BB'}dt$. Here, ρ is the density of the liquid; f is the cross-sectional area of the free rim; V_ξ is the velocity of the liquid along the rim axis S, along which the coordinate ξ is reckoned; V_r and V_θ are the radial and azimuthal components of velocity in the film over the area A'B'; h is the thickness of the film; ψ is the angle between the direction of the radius and the tangent τ_1 to the axis S. Figuring the mass balance for the rim section ABB'A', we obtain the following continuity equation for the free rim:

$$d(V_\xi f)/d\xi = h(V_r \sin\psi + V_\theta \cos\psi). \tag{1.1}$$

Examination of the momentum balance inside the rib with the assumption that here the liquid is instantaneously unloaded from internal stresses leads to the equation

$$\rho d\left(V_\xi^2 f \tau_1\right)/d\xi = \rho V h (V_r \sin\psi + V_\theta \cos\psi) + \sigma_n h + 2\alpha \mathbf{n}_1, \tag{1.2}$$

where $\mathbf{n}_1$ is a normal to S in the plane of the film; σ_n is the stress in the film on the area A'B'; α is the surface tension of the liquid.

Projecting (1.2) onto the tangent and the normal to S, we have

$$\begin{aligned} \rho \frac{dV_\xi^2 f}{d\xi} &= \rho h (V_r \sin\psi + V_\theta \cos\psi)(V_r \cos\psi - V_\theta \sin\psi) + h[\sin\psi\cos\psi(\sigma_{\theta\theta} - \sigma_{rr}) - \sigma_{r\theta}\cos 2\psi], \\ \rho V_\xi^2 f\left(\frac{d\psi}{d\xi} - \frac{d\theta}{d\xi}\right) &= -\rho h (V_r \sin\psi + V_\theta \cos\psi)^2 + \\ &+ h(\sigma_{rr}\sin^2\psi + \sigma_{\theta\theta}\cos^2\psi + \sigma_{r\theta}\sin 2\psi) + 2\alpha. \end{aligned} \tag{1.3}$$

We will use σ_{rr}, $\sigma_{\theta\theta}$, $\sigma_{r\theta}$ to denote components of the stress tensor in the film on the boundary A'B' with the free rim.

The above equations are valid only up to the beginning of the breakaway of a drop from the rim, leading to its destruction. This does not diminish their significance, since experiments show that the free rim remains intact over fairly long sections even in the case of water films.

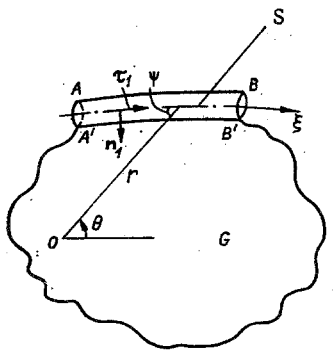

Fig. 2

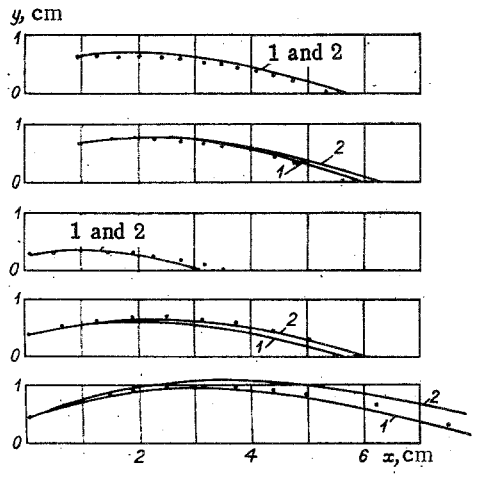

Fig. 3

The following geometric relations are added to Eqs. (1.1) and (1.3):

$$\frac{d\theta}{dr} = -\frac{1}{r}\operatorname{tg}\psi, \quad d\xi \sin\psi = -rd\theta. \tag{1.4}$$

One of the solutions of system (1.1), (1.3), and (1.4), represented in the form r = R(θ), gives the equation of the rim axis S.

In the present case of a stationary film with a plane middle surface and variable thickness, we write the general equations of motion of the liquid in the film [3, 4] in the form

$$\begin{gathered}\frac{\partial}{\partial r}(V_r rh) + \frac{\partial}{\partial\theta}(V_\theta h) = 0,\\ \rho V_r rh\frac{\partial V_r}{\partial r} + \rho V_\theta h\frac{\partial V_r}{\partial\theta} - \rho V_\theta^2 h = \frac{\partial\sigma_{rr}rh}{\partial r} + \frac{\partial\sigma_{r\theta}h}{\partial\theta} - \sigma_{\theta\theta}h,\\ \rho V_r rh\frac{\partial V_\theta}{\partial r} + \rho V_\theta h\frac{\partial V_\theta}{\partial\theta} + \rho V_\theta V_r h = \frac{\partial\sigma_{r\theta}rh}{\partial r} + \frac{\partial\sigma_{\theta\theta}h}{\partial\theta} + \sigma_{r\theta}h.\end{gathered} \tag{1.5}$$

To find the stresses σ in the film, it is necessary to use the governing rheological equations of the liquid. They will be used in a form corresponding to one of the variants of a viscoelastic Maxwell liquid [5]:

$$\begin{gathered}V_r\frac{\partial\tau_{zz}}{\partial r} + \frac{V_\theta}{r}\frac{\partial\tau_{zz}}{\partial\theta} = 2\tau_{zz}\left(-\frac{\partial V_r}{\partial r} - \frac{1}{r}\frac{\partial V_\theta}{\partial\theta} - \frac{V_r}{r}\right) - \frac{1}{\lambda}\tau_{zz} + \frac{2\mu}{\lambda}\left(-\frac{\partial V_r}{\partial r} - \frac{1}{r}\frac{\partial V_\theta}{\partial\theta} - \frac{V_r}{r}\right),\\ V_r\frac{\partial\tau_{rr}}{\partial r} + \frac{V_\theta}{r}\left(\frac{\partial\tau_{rr}}{\partial\theta} - 2\tau_{r\theta}\right) = 2\tau_{rr}\frac{\partial V_r}{\partial r} + 2\tau_{r\theta}\left(\frac{1}{r}\frac{\partial V_r}{\partial\theta} - \frac{V_\theta}{r}\right) - \frac{\tau_{rr}}{\lambda} + \frac{2\mu}{\lambda}\frac{\partial V_r}{\partial r},\\ V_r\frac{\partial\tau_{r\theta}}{\partial r} + \frac{V_\theta}{r}\left(\frac{\partial\tau_{r\theta}}{\partial\theta} + \tau_{rr} - \tau_{\theta\theta}\right) = \tau_{rr}\frac{\partial V_\theta}{\partial r} + \tau_{\theta\theta}\left(\frac{1}{r}\frac{\partial V_r}{\partial\theta} - \frac{V_\theta}{r}\right)\\ + \tau_{r\theta}\left(\frac{1}{r}\frac{\partial V_\theta}{\partial\theta} + \frac{V_r}{r} + \frac{\partial V_r}{\partial r}\right) - \frac{\tau_{r\theta}}{\lambda} + \frac{\mu}{\lambda}\left(\frac{1}{r}\frac{\partial V_r}{\partial\theta} + \frac{\partial V_\theta}{\partial r} - \frac{V_\theta}{r}\right),\\ V_r\frac{\partial\tau_{\theta\theta}}{\partial r} + \frac{V_\theta}{r}\left(\frac{\partial\tau_{\theta\theta}}{\partial\theta} + 2\tau_{r\theta}\right) = 2\tau_{r\theta}\frac{\partial V_\theta}{\partial r} + 2\tau_{\theta\theta}\left(\frac{1}{r}\frac{\partial V_\theta}{\partial\theta} + \frac{V_r}{r}\right) - \frac{\tau_{\theta\theta}}{\lambda} + \frac{2\mu}{\lambda}\left(\frac{1}{r}\frac{\partial V_\theta}{\partial\theta} + \frac{V_r}{r}\right),\\ \sigma_{rr} = \tau_{rr} - \tau_{zz},\ \sigma_{\theta\theta} = \tau_{\theta\theta} - \tau_{zz},\ \sigma_{r\theta} = \tau_{r\theta},\end{gathered} \tag{1.6}$$

where τ_{zz}, τ_{rr}, $\tau_{\theta\theta}$, and $\tau_{r\theta}$ are the deviator stresses in the film; μ and λ are the viscosity and relaxation time of the liquid. Similar rheological relations are obtained from molecular-hydrodynamic models [6] if the cumulative elastic strains are not too great.

The presence of free rims may have an effect on flow inside the film. Thus, the equations of film dynamics (1.5)-(1.6) should be solved simultaneously with the equations of the rim in region G with unknown boundary S corresponding to free rims. These equations are solved with suitable conditions on the discharge line and S. Below we examine a simplified variant of this problem, assuming that the rib does not have an inverse effect on flow in the film. In this case, flow in the film can in principle be examined independently, and we are concerned only with finding the unknown position of the rims. This physically formulated assumption rests on two facts. First, the liquid always flows from the film to the rim (the

reverse situation is not seen). Second and most important, here we are examining only fairly rapid flows (or liquids with sufficiently low viscosity) in which perturbations are propagated mostly along the flow. Propagation of perturbations across the flow is limited to the narrow boundary layers. The character of these layers is similar to that examined in [7] in an analysis of the formulation of boundary conditions on the far end of a free film.

The velocity component in the film which is tangent to the free rim $V_{\xi 1} = V_r \cos\psi - V_\theta \sin\psi$ differs from the liquid velocity in it V_ξ. Thus, a mixing layer should develop on the boundary between the free rim and film A'B', this layer intensifying the equalization of velocities in the free rim.

2. Free Rims with Radial Flow in a Film. We assume that flow in the film is purely radial. Meanwhile, it follows from the continuity condition that

$$V_r = C/[rh(r)],\ V_\theta = 0,\ C = \text{const}.$$

Experiments show that the character of flow in the film is usually radial not only when the film is formed on an axisymmetric obstacle [7], but also in the case of discharge of a film from a slit nozzle.

Then, with allowance for (1.4), we obtain the following from the continuity equation for the rim (1.1)

$$V_\xi f = Q_1 + C(\theta_0 - \theta), \tag{2.1}$$

where Q_1 is the flow rate in the initial section of the rib corresponding to the angle θ_0.

Using Eq. (2.1), we can simplify Eqs. (1.3) and (1.4) and change them to dimensionless form

$$\frac{dV_\xi}{dr} = \frac{1}{q_1 + \theta_0 - \theta}\left\{\sin\psi\left[\frac{V_r}{r} + \frac{1}{V_r r}(\sigma_{\theta\theta} - \sigma_{rr})\right] - \frac{V_\xi \operatorname{tg}\psi}{r}\right\},$$
$$\frac{d\psi}{dr} = -\frac{\operatorname{tg}\psi}{r} + \frac{1}{V_\xi(q_1 + \theta_0 - \theta)}\left[-\frac{V_r \sin^2\psi}{r\cos\psi} + \frac{1}{\mathrm{We}\cos\psi} + \frac{1}{V_r r\cos\psi}(\sigma_{rr}\sin^2\psi + \sigma_{\theta\theta}\cos^2\psi)\right],\ \frac{d\theta}{dr} = -\frac{\operatorname{tg}\psi}{r}. \tag{2.2}$$

The corresponding equations for flow in the film take the form

$$\frac{dV_r}{dr} = \left[1 - V_r^{-2}(\tau_{rr} + 4\mathrm{K} + 3\tau_{zz})\right]^{-1}\left[V_r^{-2}(-\mathrm{K}\,\mathrm{Re}\,\tau_{rr} + 2\tau_{zz}V_r/r + \mathrm{K}\,\mathrm{Re}\,\tau_{zz} + 2\mathrm{K}V_r/r) - (\tau_{\theta\theta} - \tau_{zz})/(rV_r)\right],$$
$$\frac{d\tau_{zz}}{dr} = \frac{1}{V_r}\left[-2\tau_{zz}\left(\frac{dV_r}{dr} + \frac{V_r}{r}\right) - \mathrm{K}\,\mathrm{Re}\,\tau_{zz} - 2\mathrm{K}\left(\frac{dV_r}{dr} + \frac{V_r}{r}\right)\right],$$
$$\frac{d\tau_{rr}}{dr} = \frac{1}{V_r}\left[2\tau_{rr}\frac{dV_r}{dr} - \mathrm{K}\,\mathrm{Re}\,\tau_{rr} + 2\mathrm{K}\frac{dV_r}{dr}\right], \tag{2.3}$$
$$\frac{d\tau_{\theta\theta}}{dr} = \frac{1}{V_r}\left[\frac{2\tau_{\theta\theta}V_r}{r} - \mathrm{K}\,\mathrm{Re}\,\tau_{\theta\theta} + 2\mathrm{K}\frac{V_r}{r}\right],$$
$$\sigma_{rr} = \tau_{rr} - \tau_{zz},\ \sigma_{\theta\theta} = \tau_{\theta\theta} - \tau_{zz},$$
$$\mathrm{We} = \frac{\rho h_0 V_0^2}{2\alpha},\ \mathrm{K} = \frac{\mu}{\rho\lambda V_0^2},\ \mathrm{Re} = \frac{r_0 V_0 \rho}{\mu},\ q_1 = \frac{Q_1}{r_0 V_0 h_0}.$$

In Eqs. (2.2) and (2.3), the velocities are referred to V_0, the radius is referred to r_0, and the stresses are referred to ρV_0^2.

Equations similar to (2.3) were written in [2] (see [1] also) for an ideal liquid, when $V_r \equiv 1$, $\sigma_{rr} = \sigma_{\theta\theta} \equiv 0$. Meanwhile, the initial flow rate in the rib q_1 was assumed to be zero; the solutions of these equations were evidently not studied.

By integrating Eqs. (2.3) with initial conditions written in the initial section of the film r = 1, we can find all of the flow parameters in the film that are needed to find the rim axis S. The form of this axis and the flow parameters in the rim are then determined from Eqs. (2.2).

The question of formulating the initial conditions for these equations is important. There are two fundamentally different cases: From the beginning we have had a problem concerning a boundary stream with a nontrivial flow rate q_1; the second case involves a boundary stream which forms at the site of discontinuity of film ($q_1 = 0$). The first situation is

clearly realized in the discharge of a stream from a slit die with a dumbbell-shaped cross section or in the event of discontinuity of the film caused by a wide obstacle. The second situation is realized in the event of discontinuity of the film as a result of the presence of a very fine wire. In fact, in the flow of a film against an obstacle of width d, we have the obvious estimate for the flow rate in the initial section of the free rim $(1/2)V_*h_*d$ (the asterisks denote values at the location of the obstacle): Accordingly, $q_1 = d/(2r_1)$, and for an obstacle of sufficiently small size $q_1 \to 0$.

In the first case, it is necessary to assign the values of q_1, ψ_0, and $V_{\xi 0}$ in the initial section of the boundary stream, while in the second case it is necessary to assign the initial point $r = r_1$, $\theta = \theta_0$ — particularly for Eqs. (2.2). It can be shown that ψ and V_ξ in (2.2) take finite values for $r = r_1$, $q_1 = 0$ only with satisfaction of the conditions

$$r = r_1,\ V_\xi = V_{\xi 0},\ \psi = \psi_0,\ \theta = \theta_0,$$
$$V_{\xi 0} = \left(V_r + \frac{\sigma_{\theta\theta} - \sigma_{rr}}{V_r}\right)\cos\psi, \tag{2.4}$$
$$\sin^2\psi_0 = \left(\frac{1}{We} + \frac{\sigma_{\theta\theta}}{V_r}\right)\Big/\left(V_r + \frac{\sigma_{\theta\theta} - \sigma_{rr}}{V_r}\right)$$

(the ambiguity of the solution of the equation for the angle reflects the fact that two streams are formed when the flow is disrupted by an obstacle). Accordingly, dV_ξ/dr and $d\psi/dr$ also take finite values at $r = r_1$.

The value of the radius $r = r_2$ at which

$$V_r^2 - rV_r/We - \sigma_{rr} = 0 \tag{2.5}$$

corresponds to the creation of a free rim in the form of an arc (a condition analogous to (2.5) for an ideal liquid was obtained in [2]). The liquid in this rim is relieved of surface and elastic forces, while the separation of a drop from it leads to destruction of the film at $r = r_2$. In a number of cases, free rims which develop on fine wires or on a nozzle edge cannot close the radius $r = r_2$, and the film turns out to be fairly long and bounded by three free rims. By analogy with gas dynamics, free rims which begin on obstacles or on a nozzle edge can be called "oblique discontinuities," while free rims in the form of arcs of a circle at $r = r_2$ can be called "normal discontinuities."

3. Experiment and Comparison of Its Results with the Theory. To check the adequacy of the theoretical scheme devised here, we performed calculations for films of an ideal liquid (water) and compared the results with an experiment.

In the experiment, we used thin wires to isolate a thin sector from a film created by a slit die. The sector itself constituted a plane film delimited by boundary streams (see Fig. 1b). The velocity field V in the film was found by the method of tracing hydrogen bubbles in combination with photographs taken with stroboscopic illumination; the distribution of the unit volumetric flow rate in the film, equal to Vh, was found independently. This allowed us to find V and h separately and confirm the constancy of V and the radial character of the flow.

The calculations involved integration of Eq. (2.2) with the corresponding initial conditions. Here, in the ideal liquid the stresses σ_{rr} and $\sigma_{\theta\theta}$ were assumed to be zero, while the velocity $V_r \equiv 1$.

Figure 3 shows the form of the rims which are created with different initial positions of the wires that cut the film (different r_1). The points represent experimental results, while curves 1 show the calculated results; we assumed that $q_1 = 0$ and we used the initial conditions (2.4), since in this case an estimate of the initial flow rate in the boundary stream gives values $q_1 \sim (3\text{-}6)\cdot 10^{-3}$. The Ox axis is the symmetry axis of the flow.

In the present case, the angles made by the rib with the symmetry axis of the film are small; this makes it possible to simplify the equation of the rim additionally by representing it in the form

$$\left(1 - \theta_0^{-1}\frac{y}{x} + \frac{m_0}{y_0\rho h_0}\right)\frac{d^2y}{dx^2} = \theta_0^{-1}xV_0^2\left(\frac{y}{x^2} - \frac{dy}{dx}\frac{1}{x}\right)^2 - \frac{1}{\rho V_0^2 h_0 y_0}\left(\frac{\sigma_{\theta\theta}h_0x_0}{x} + 2\alpha\right), \tag{3.1}$$

where x and y are Cartesian coordinates ($x = r\cos\theta$, $y = r\sin\theta$); $m_0 = f_0\rho$ is the mass of the liquid in the initial element of a rim of unit length at the point of formation of the free

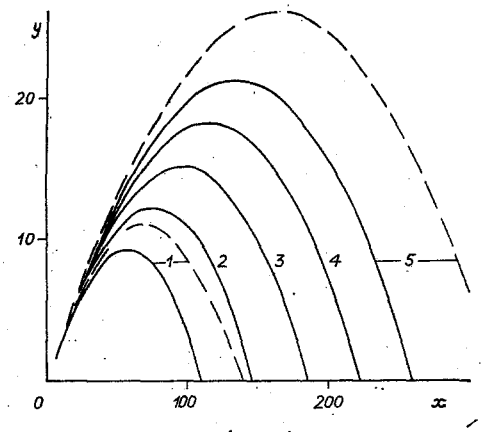

Fig. 4

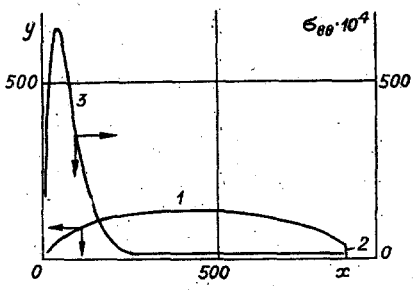

Fig. 5

rim; h_0 is the thickness of the film at this point; x_0, y_0 ($\theta_0 = y_0/x_0$) are the coordinates of this point; V_0 is the velocity of the liquid flow in the film, which coincides in the given formulation with the velocity of the liquid flow in the rim.

Asymptotic equation (3.1) is valid under the conditions $\theta_0 \ll 1$, $\rho V^2 \gg \sigma_{\theta\theta}$, $\rho V^2 \gg \sigma_{rr}$. It is convenient in the sense that it makes it possible to solve the inverse problem — find the azimuthal stresses in the film $\sigma_{\theta\theta}$ from the form of the rim. Equation (3.1) should be integrated with allowance for the second condition of (2.4).

To evaluate the error introduced by changing over to asymptotic equation (3.1), we used it to calculate the form of films for the test conditions shown in Fig. 3 (line 2 represents the calculated results). It is evident that asymptotic equation (3.1) agrees satisfactorily with the experimental results for sufficiently small values of θ_0. In [1], an explicit approximate expression for the form of the rim $r = R(\theta)$ was obtained from (2.2) for small angles of inclination of free rims relative to the symmetry axis of films.

In the next stage of the experiment, we studied films of dilute polymer solutions and attempted to determine the stresses in the liquid by means of Eq. (3.1). However, the results obtained were not sufficiently accurate, so we subsequently used another method.

Calculations were performed with the Maxwell model of a viscoelastic liquid and values of the parameters $\mu = 10^{-3}$ kg/(m·sec) and $\lambda \sim 10^{-2}$ sec, which are typical for dilute polymer solutions. It was found that this model predicts that the form of the free rims is independent of the elastic properties of the dilute solution and that the stresses $\sigma_{\theta\theta} \sim 1$ N/m^2.

Let us examine the results obtained in the calculation of flows from slit nozzles on the basis of Eqs. (2.2) and (2.3). Figure 4 shows data for a viscoelastic liquid issuing from a slit nozzle in the case of developed boundary streams at the edge of the nozzle. Here, we took $q_1 = 0.1$, $r_1 = 5$, $\psi_0 = 0$, $\theta_0 = 15°$, and $V_{\xi 0} = V_r(r_1)$ (nozzle with dumbbell-shaped cross section). We used r_0 as the length scale, and we assumed that at $1 \leqslant r \leqslant r_1$ flow in the nozzle develops as a free film. Friction losses on the wall are negligible. At $1 \leqslant r \leqslant r_1$, Eqs. (2.3) are integrated with the initial conditions $r = 1$, $V_r = 1$, and $\tau_{zz} = \tau_{rr} = \tau_{\theta\theta} = 0$. At $r > r_1$, Eqs. (2.3) are integrated together with Eqs. (2.2). The solid lines 1-5 in Fig. 4 correspond to $We = 0.36\cdot 10^5$, $Re = 6$, $K = 0.278\cdot 10^{-4}$; $We = 0.64\cdot 10^5$, $Re = 8$, $K = 0.156\cdot 10^{-4}$; $We = 10^5$, $Re = 10$, $K = 10^{-5}$; $We = 1.44\cdot 10^5$, $Re = 12$, $K = 0.69\cdot 10^{-5}$; $We = 1.96\cdot 10^5$, $Re = 14$, $K = 0.51\cdot 10^{-5}$ (the initial velocity of the liquid increases while the other parameters remain fixed). For example, the parameter values for curve 3 in Fig. 4 correspond to a monotonic increase in the stress $\sigma_{\theta\theta}$ along the film until it joins the free rims — the lifetime of a liquid particle in the film is too short for any appreciable relaxation of the azimuthal stresses.

The parameter values adopted here pertain to a region in which the elastic forces are intentionally more important than the surface forces. Thus, the form of the film is completely determined by the elastic modulus of the liquid. A decrease in the latter is accompanied by a decrease in the elastic forces, which leads to greater divergence of the free rims. The rims converge more rapidly with an increase in the modulus. The dashed curves 1 and 5 in Fig. 4 show results for an elastic modulus which has been reduced by a factor of 1.5 (with a corresponding reduction in K); the rest of the dimensionless criteria have the same values as before.

With a decrease in the initial flow rate q_1, the boundary stream formed in the case of discharge from a slit nozzle with a dumbbell shape becomes more and more like the boundary stream formed on the edge of a nozzle in the form of a highly prolate ellipse, when $q_1 = 0$ and initial conditions (2.4) are valid.

Finally, let us examine data pertaining to fairly long films bounded by three free rims. Figure 5 shows in dimensionless form the results of calculation of discharge from a slit nozzle with a dumbbell-shaped edge (We = 10^3, Re = $0.28 \cdot 10^3$, K = 10^{-4}, $q_1 = 0.1$, $r_1 = 5$, $\theta_0 = 60°$). Curve 1 is for one of two free rims beginning on the nozzle edge ("oblique discontinuity), curve 2 is for a free rim with an axis in the form of a circle arc ("normal discontinuity"), and curve 3 is the distribution of the azimuthal stress $\sigma_{\theta\theta}$ along the film. The maximum of this stress and the subsequent sharp reduction are due to relaxation. For the parameter values corresponding to Fig. 4, the film becomes longer and a third rim develops behind it as a result of an increase in the divergence angle θ_0.

It can be suggested that the appearance of a third free "unloading rim" in the formal solution before joining of the boundary streams corresponds physically to breakdown of the film.

LITERATURE CITED

1. C. I. Clark and N. Dombrowski, "The dynamics of the rim of a fan spray sheet," Chem. Eng. Sci., 26, No. 11 (1971).
2. G. Taylor, "The dynamics of thin sheets of fluid. II. Waves on fluid sheets," Proc. R. Soc. London, A253, No. 1274 (1959).
3. V. M. Entov, Dynamics of Films of Viscous and Elastic Liquids, Preprint IPM Akad. Nauk SSSR, No. 130 (1979).
4. V. M. Entov, "On the dynamics of films of viscous and elastoviscous liquids," Arch. Mech., 34, No. 4 (1982).
5. G. Astarita and G. Marrucci, Principles of Non-Newtonian Fluid Mechanics, McGraw-Hill, New York (1974).
6. E. J. Hinch, "Mechanical models of dilute polymer solutions in strong flows," Phys. Fluids, 20, No. 10, Pt. 2 (1977).
7. V. M. Entov, Kh. S. Kestenboim, et al., "Dynamic mode of equilibrium of films of viscous and viscoelastic fluids," Izv. Akad. Nauk SSSR, Mekh. Zhidk. Gaza, No. 2 (1980).

NONSYMMETRIC COLLISION OF PLANE JETS OF AN IDEAL INCOMPRESSIBLE FLUID

S. A. Kinelovskii and A. V. Sokolov

UDC 532.522.2

The problem of the nonsymmetric collision of plane jets of an ideal incompressible liquid has been regarded for several decades as not having an unambiguous solution (see [1-3], for example). The reason for the ambiguity is the mathematical indeterminacy of the problem, although it could be expected that with given values of the width of the colliding streams and the angle of impact, the configuration of the flow should be unambiguously determined. The interest in this problem stems from the fact that it is widely used to describe (in a first approximation) the high-speed oblique collision of metal plates.

Figure 1 shows the flow pattern in the collision of plane free jets having the same density $\rho = 1$ and velocity $v = 1$ (at an infinitely distant point and on the free boundaries). Here, a_1 and a_3 are the widths of the colliding jets (at the infinitely distant point), θ_3 is the angle of impact, a_2 and a_4 are the widths of the outgoing jets, and θ_2 and θ_4 are the angles of their inclination to the x axis (for simplicity, the angle θ_4 has been reduced by π). Three equations follow from the conditions of mass conservation for the flow and projections of the momentum flow. With allowance for the adopted notation, these equations take the form

$$a_1 + a_3 = a_2 + a_4, \quad a_1 + a_3 \cos\theta_3 = a_2 \cos\theta_2 - a_4 \cos\theta_4, \quad a_3 \sin\theta_3 = a_2 \sin\theta_2 - a_4 \sin\theta_4. \tag{1}$$

Novosibirsk. Translated from Zhurnal Prikladnoi Mekhaniki i Tekhnicheskoi Fiziki, No. 1, pp. 54-57, January-February, 1986. Original article submitted October 26, 1984.

0021-8944/86/2701-0047$12.50